

Collective dynamics in a one-dimensional Heisenberg ferromagnetic spin chain

R. Arun,^{1, 2, a)} M. Lakshmanan,^{3, b)} and Avadh Saxena^{4, c)}

¹⁾ *Center for Nonlinear and Complex Networks, SRM TRP Engineering College, Tiruchirappalli-621 105, Tamil Nadu, India.*

²⁾ *Centre for Research, Trichy SRM Medical College Hospital and Research Center, Tiruchirappalli 621 105, Tamil Nadu, India.*

³⁾ *Department of Nonlinear Dynamics, Bharathidasan University, Tiruchirappalli - 620024, India.*

⁴⁾ *Theoretical Division and Center for Nonlinear Studies, Los Alamos National Laboratory, NM 87545, USA*

(Dated: 9 June 2026)

We investigate the different oscillatory modes, namely, complete synchronization, inphase synchronization, antiphase synchronization and desynchronization in a one-dimensional anisotropic Heisenberg ferromagnetic spin chain consisting of a large number of spins. By solving the associated Landau-Lifshitz-Gilbert-Slonczewski equation for the spins we show the simultaneous existence of the above mentioned oscillatory modes in the spins. We observe that when the number of the spins is large the synchronization is lost between the spins; however, we identify that the field-like torque is able to induce synchronous oscillations of the spins in the chain again. We also confirm the agreement of the numerically obtained values of the frequency of the inphase synchronized oscillations with the analytically obtained values.

^{a)}Electronic mail: arunbdu@gmail.com

^{b)}Electronic mail: lakshman.cnld@gmail.com

^{c)}Electronic mail: avadh@lanl.gov

I. INTRODUCTION

Understanding the intrinsic localized modes and associated oscillations of different types in the context of classical nonlinear Hamiltonian spin lattices has been a fundamentally interesting topic. The investigation on the dynamics of classical Heisenberg ferromagnetic spin chain has always been a problem of substantial interest. Anisotropic Heisenberg ferromagnetic spin system is one of the important discrete nonlinear dynamical systems which has received considerable attention in diverse areas of physics for a long time. Obtaining exact solutions for discrete nonlinear physical systems remains a significant and challenging problem of current research interest. In the continuum limit, the one-dimensional Heisenberg ferromagnetic spin system with nearest-neighbor exchange interaction is known to give rise to several completely integrable systems that support soliton solutions. For instance, the pure isotropic system¹⁻³, the uniaxial anisotropic system^{4,5} and the biaxial anisotropic system⁶ all turn out to be completely integrable infinite dimensional nonlinear systems.

Apart from a variant called Ishimori spin chain there are no other exactly solvable discrete dynamical Heisenberg spin systems that have been identified in the literature. The Ishimori spin chain is a completely integrable system⁷. In contrast, two of the present authors⁸ have shown that the discrete lattice system, incorporating onsite anisotropy and an external magnetic field, admits several classes of exact solutions expressed through Jacobian elliptic functions⁸. The emergence of intrinsic localized breathers in appropriately anisotropic ferromagnetic spin chains is of considerable practical relevance^{9,10}. In recent years, significant attention has been devoted to the identification and analysis of intrinsic localized modes (ILMs), or discrete breathers, in classical nonlinear Hamiltonian lattices, including magnetic chains¹¹⁻²². ILMs are dynamical localized states, which include periodic oscillations in time in a localized space. Though the analytical solution for the discrete system with onsite anisotropy and an external magnetic field is available, a solution for the anisotropic ferromagnetic spin chain with external magnetic field along with damping is unavailable.

Here, we delve into the different dynamical states present in the anisotropic Heisenberg ferromagnetic spin chain system. Starting from the Hamiltonian associated with the lattice corresponding to the Heisenberg spin chain we solve numerically the associated Landau-Lifshitz-Gilbert-Slonczewski (LLGS) equation, which includes the spin-transfer-torque effect on the spins associated with the lattice. We prove the existence of self oscillations, i.e.

oscillations without any periodic input on the spins in the chain. By numerically solving the LLGS equation obtained for the N number of spins with nearest neighbour interaction we identify different dynamical states associated with the spin chain system. Specifically, we identify different kinds of oscillations in the chain, namely (i) completely synchronized oscillations, (ii) inphase synchronized oscillations, (iii) antiphase synchronized oscillations and (iv) desynchronized oscillations by changing the direction of external field in the presence of field-like torque. We observe the simultaneous existence of the above oscillatory modes in the chain consisting of N number of spins. The synchronization between the different pairs of the spins is confirmed by the standard deviation and phase difference between them. The numerical results are validated with the frequency of the oscillations derived analytically. We confirm that when the field-like torque is incorporated in the chain, the spins are expected to show inphase synchronized oscillations from desynchronized oscillations.

The plan of the paper is as follows: The model of the spin system is discussed in Sec. II, where the LLGS equation corresponding to the Heisenberg ferromagnetic spin chain is derived from the respective Hamiltonian of the lattice. In Sec. III, the existence of different modes of oscillations including complete synchronized, inphase synchronized, antiphase synchronized and desynchronized oscillations are investigated. The main results are summarized and concluded in Sec. IV.

II. MODEL

The Hamiltonian corresponding to the evolution of N number of spins of a one-dimensional anisotropic Heisenberg ferromagnetic spin chain is given by

$$\mathcal{H} = - \sum_{i=1}^N [A S_i^x S_{i+1}^x + B S_i^y S_{i+1}^y + C S_i^z S_{i+1}^z] - K_z \sum_{i=1}^N (S_i^z)^2 - \mathbf{H} \cdot \sum_{i=1}^N \mathbf{S}_i, \quad (1)$$

where i runs from 1 to N . In Eq. (1), A , B and C are exchange interaction constants, while K_z is an onsite anisotropy parameter along the z -direction. Further, $\mathbf{H} = H_x \mathbf{e}_x + H_y \mathbf{e}_y + H_z \mathbf{e}_z$ is the external field. Here, \mathbf{e}_x , \mathbf{e}_y , and \mathbf{e}_z are the unit vectors along the positive x , y , and z directions, respectively. Eq. (1) can be rewritten as

$$\mathcal{H} = - \sum_{i=1}^N [A S_i^x S_{i+1}^x + B S_i^y S_{i+1}^y + C S_i^z S_{i+1}^z] - K_z \sum_{i=1}^N (S_i^z)^2 - H_x \sum_{i=1}^N S_i^x - H_y \sum_{i=1}^N S_i^y - H_z \sum_{i=1}^N S_i^z. \quad (2)$$

After expanding the Hamiltonian, given in Eq. (2), around the k -th spin we get

$$\begin{aligned}
\mathcal{H} = & - [\dots + A S_{k-1}^x S_k^x + A S_k^x S_{k+1}^x + B S_{k-1}^y S_k^y + B S_k^y S_{k+1}^y + C S_{k-1}^z S_k^z + C S_k^z S_{k+1}^z + \dots] \\
& - K_z [\dots + (S_{k-1}^z)^2 + (S_k^z)^2 + (S_{k+1}^z)^2 + \dots] - H_x [\dots + S_{k-1}^x + S_k^x + S_{k+1}^x + \dots] \\
& - H_y [\dots + S_{k-1}^y + S_k^y + S_{k+1}^y + \dots] - H_z [\dots + S_{k-1}^z + S_k^z + S_{k+1}^z + \dots].
\end{aligned} \tag{3}$$

The effective field for the k -th spin can be obtained from the Hamiltonian as

$$\begin{aligned}
H_{eff,k}^x &= -\frac{\delta\mathcal{H}}{\delta S_k^x} = A(S_{k-1}^x + S_{k+1}^x) + H_x, \\
H_{eff,k}^y &= -\frac{\delta\mathcal{H}}{\delta S_k^y} = B(S_{k-1}^y + S_{k+1}^y) + H_y, \\
H_{eff,k}^z &= -\frac{\delta\mathcal{H}}{\delta S_k^z} = C(S_{k-1}^z + S_{k+1}^z) + 2K_z S_k^z + H_z.
\end{aligned}$$

By considering the one-dimensional spin chain in the free layer of a spin-valve (tri-layer) structure, the dynamics of the n -th spin in the presence of current is governed by the following LLGS equation^{23,24}

$$\frac{d\mathbf{S}_k}{dt} = -\gamma \mathbf{S}_k \times \mathbf{H}_{eff,k} - \alpha \mathbf{S}_k \times (\mathbf{S}_k \times \mathbf{H}_{eff,k}) + j \mathbf{S}_k \times (\mathbf{S}_k \times \mathbf{S}_p) + j \beta \mathbf{S}_k \times \mathbf{S}_p. \tag{4}$$

In Eq. (4) the effective field of the k -th spin $\mathbf{H}_{eff,k}$ is defined as $\mathbf{H}_{eff,k} = H_{eff,k}^x \mathbf{e}_x + H_{eff,k}^y \mathbf{e}_y + H_{eff,k}^z \mathbf{e}_z$. Here, γ is the gyromagnetic ratio, α is the damping constant, j and β are the strengths of spin-transfer torque and field-like torque, respectively.

III. SELF-OSCILLATIONS

In the absence of anisotropy, Eq.(4) has analytically been solved for the single spin by the present authors²³. However, it is hard to be solved analytically in the present form even for a single spin. Hence, in the following, the dynamics of the N spins is numerically investigated using the Runge-Kutta-4 method and also by using Mathematica.

A. Complete and inphase synchronized oscillations

Here, we show the existence of self-oscillations, that is oscillations in the absence of any external periodic source, of the spins in the one-dimensional chain. The self-oscillations of the spins are demonstrated here for the values of the parameters $A = 2, B = 2, C = 1, \gamma =$

1.0, $K_z = 0.1$, $H_x = 0.1$, $H_y = 0$, $H_z = 0$, $\alpha = 0.005$, $j = 0.1$, $\beta = 0$, and the condition $\mathbf{S}_p = \mathbf{e}_x$, corresponding to the case where the fixed polarized vector \mathbf{S}_p is parallel to the x -axis. In Fig. 1(a-f) we have plotted the evolution of x -components (S^x) for the number of spins 1, 2, ..., 6, respectively. From the figures we can observe that when the total number of spins is 4 and below ($N \leq 4$), no oscillations are exhibited and only steady states are possible. However, steady oscillations are exhibited while the total number of spins is above 4 ($N > 4$) as shown in Figs. 1(e) and (f). From Figs. 1(e-f) we can notice that the pair of spins ($i, N + 1 - i$) exhibit synchronized oscillations. The amplitudes of the oscillations of spins 1, 2, and 3 are slightly different while their frequencies are the same.

To investigate the dynamics for a large number of spins, the time evolution of S^x is plotted for 25, 30, and 100 number of spins in Figs. 2(a-c). As we can see from Figs. 2(a-c), the synchronization is lost in the oscillations when the number of spins is increased above 25 and the spins oscillate desynchronously. For the strength of the field-like torque $\beta = -0.6$, the spins exhibit inphase synchronized oscillations as shown in Fig. 2(d). This implies the possibility of getting synchronization due to the field-like torque. The frequency of oscillations of the 100 spins are the same and the amplitudes of the oscillations are different. The time evolution of S^x of 100 spins is plotted for $\beta = 0$ and $\beta = -0.6$ in Figs. 2(e) and (f), respectively. Fig. 2(e) confirms the desynchronization in oscillations of the spins and in Fig. 2(f) we can observe the inphase synchronization between the spins due to the field-like torque. Also, we can verify the complete synchronization between ($i, N + 1 - i$) spins due to the field-like torque. This complete synchronization is visualized in Fig. 3, where the time evolution of the spins 10, 91, 25, and 76 are plotted for S^x and S^z in Fig. 3(a) and (b), respectively, and we can notice that the oscillations of the spins 10 and 91 as well as 25 and 76 are completely synchronized.

To verify the complete synchronization between all the pair of spins (1,100), (2,99), (3,98), ... , (100,1) the standard deviation between their respective $S^x(t)$ is calculated and plotted in Figs. 4(a) and (b) for $\beta = 0$ and $\beta = -0.6$, respectively. The standard deviation between the j -th and k -th spins can be calculated during the time between $t = t_1$ and $t = t_2$, which is given as

$$\sigma = \frac{1}{t_2 - t_1} \sum_i \sqrt{\frac{[S_j^x(t_i) - \mu^x(t_i)]^2 + [S_k^x(t_i) - \mu^x(t_i)]^2}{2}} \quad (5)$$

where $t_i = t_1, t_1 + h, t_1 + 2h, \dots, t_2$. Here h is the step size in the computation and

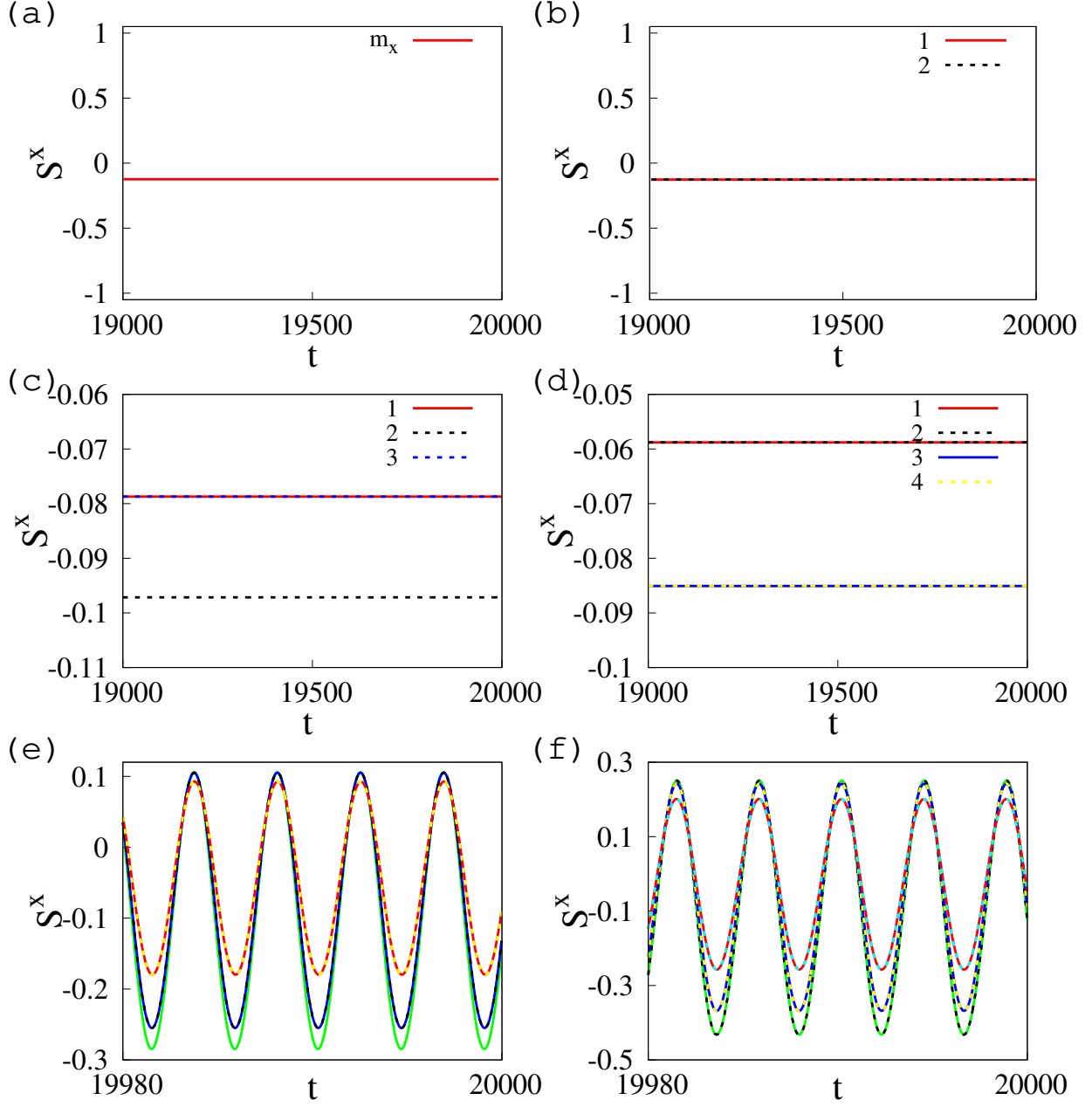


FIG. 1. Time evolution of S^x for the number of spins (a) 1, (b) 2, (c) 3, (d) 4, (e) 5, and (f) 6 for $\beta = 0$. The color codes: (e) spins 1 (solid red), 2 (solid blue), 3 (solid green), 4 (dashed black), and 5 (dashed yellow). (f) Spins 1 (solid red), 2 (solid blue), 3 (solid green), 4 (dashed black), 5 (dashed yellow), and 6 (dashed cyan).

$$\mu^x(t_i) = (S_j^x(t_i) + S_k^x(t_i))/2.$$

In Fig. 4(a) and (b), where the standard deviation σ is plotted for $\beta = 0$ and -0.6 , respectively, the white regions in Figs. 4(a) and (b) correspond to $\sigma > 1.0$ and $\sigma > 0.01$,

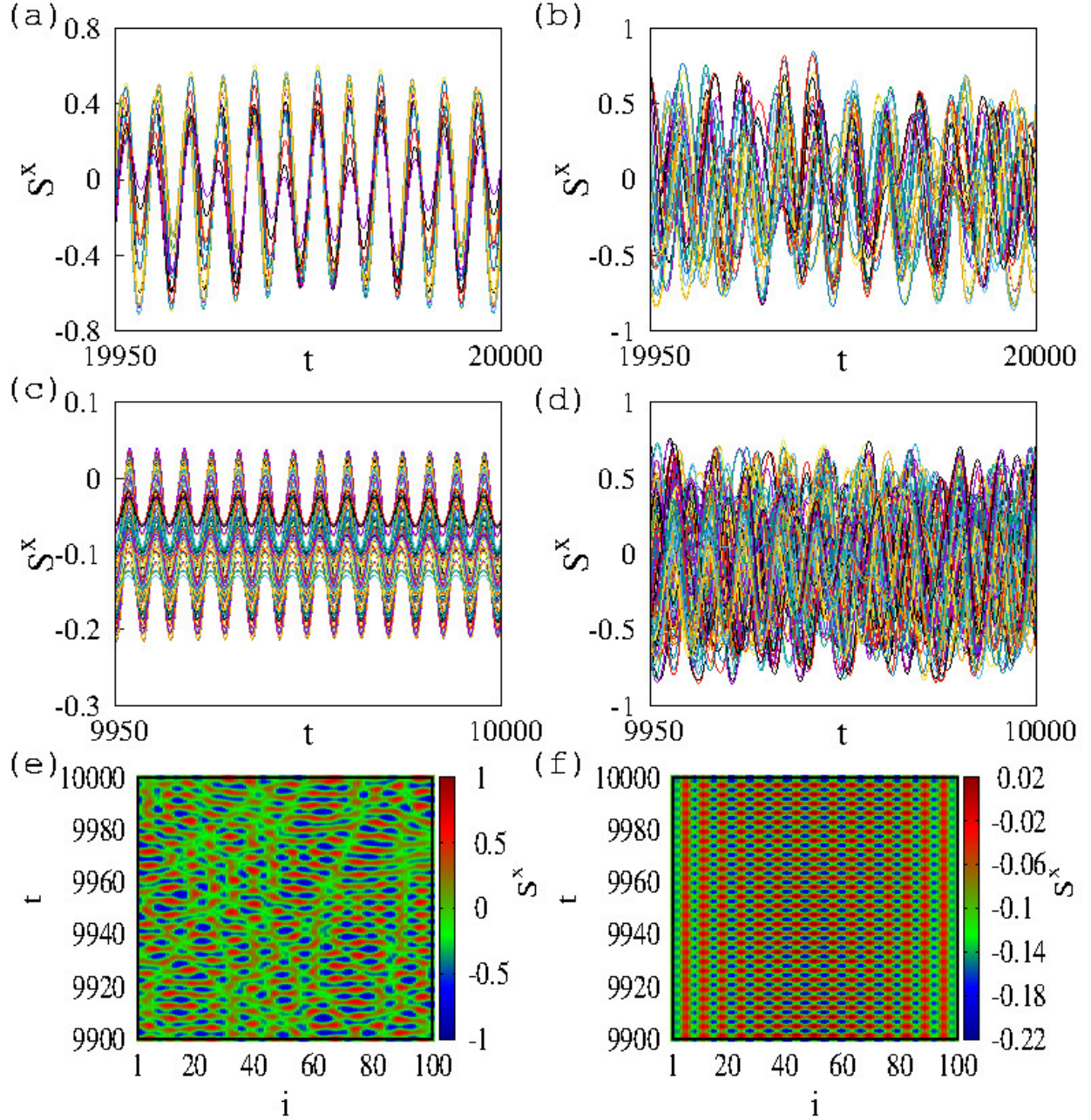


FIG. 2. Time evolution of S^x when $\beta = 0$ for the number of spins N (a) 25, (b) 30, (c) 100 and for (d) 100 when $\beta = -0.6$. Time evolution of 100 spins when (e) $\beta = 0$ and (f) $\beta = -0.6$.

respectively. In Figs. 4(a) we can observe that the standard deviation is quite high between any pair of spins in the chain for $\beta = 0$. When $\beta = -0.6$, the standard deviation σ between the spins $(i, N + 1 - i)$ is close to zero as shown in Fig. 4(b). This implies that these pairs of spins are exhibiting completely synchronized oscillations due to the field-like torque.

From Figs. 4(a) and (b) we can understand that the spins $(i, N + 1 - i)$ are exhibiting

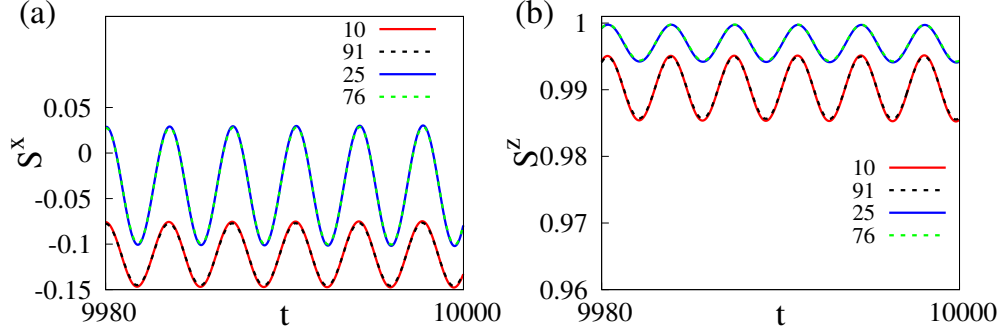


FIG. 3. Complete synchronization between the spins (10,91) and (25,76) in their time evolution of (a) S^x , and (b) S^z when $\beta = -0.6$.

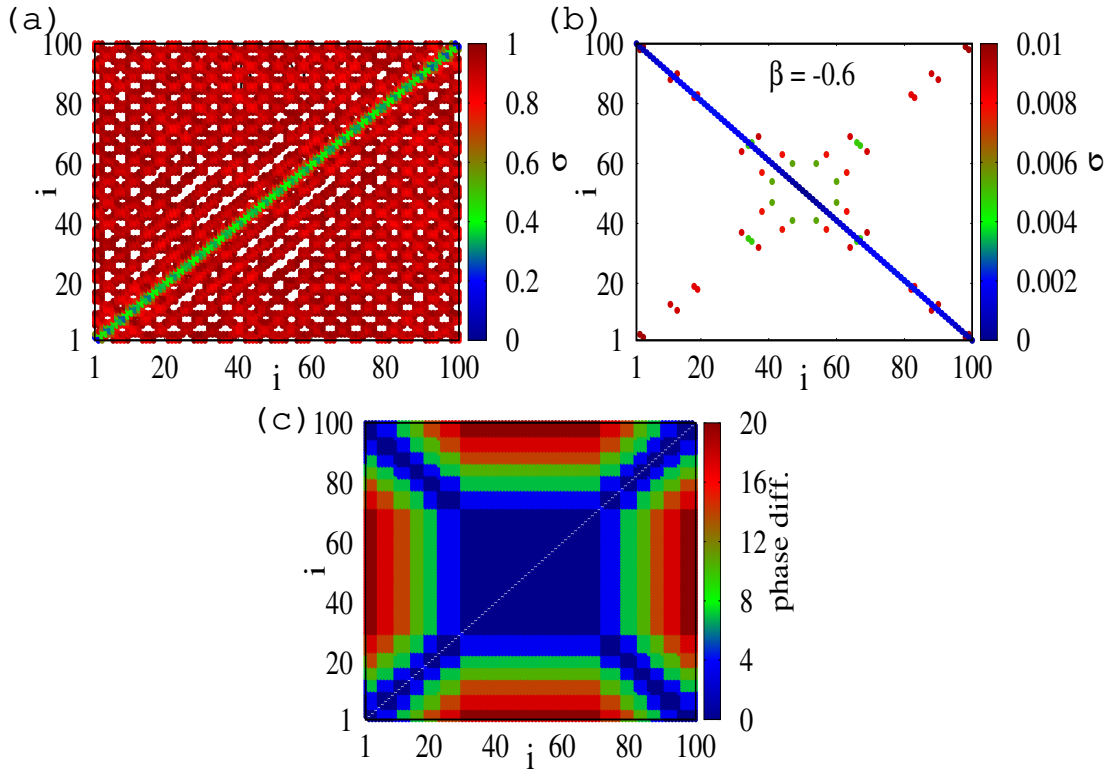


FIG. 4. The standard deviation estimated for $S^x(t)$ between different pairs of spins ' i ' and ' $N+1-i$ ' for (a) $\beta = 0$ and (b) $\beta = -0.6$. (c) Phase difference in degrees between different the pairs of spins when $\beta = -0.6$. Here, $H_x = 0.1, H_y = 0, H_z = 0, I = 0.1$.

complete synchronization. The remaining pairs of spins other than $(i, N + 1 - i)$ oscillate with inphase synchronization. In Fig. 4(c), the pair-wise phase difference has been plotted and this exhibits that the spins oscillate with inphase synchronization even though they do

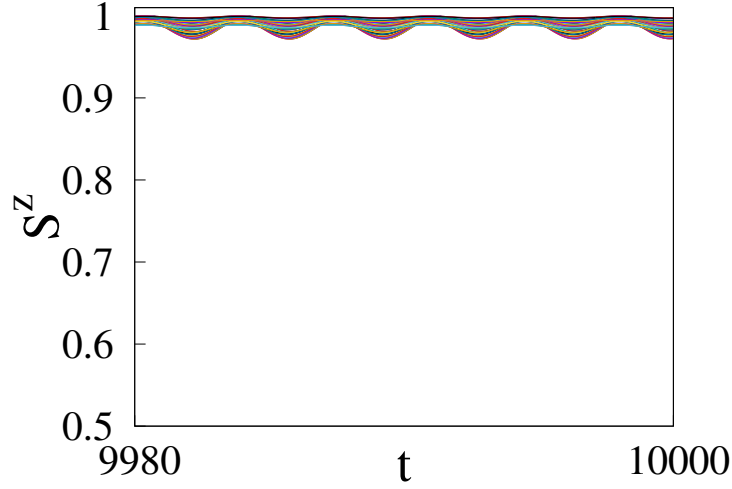


FIG. 5. Time evolution of S^z of 100 number of spins for the parameters $A = 2, B = 2, C = 1, K_z = 0.1, H_x = 0.1, H_y = 0, H_z = 0, j = 0.1, \gamma = 1.0, \alpha = 0.005, \beta = -0.6$.

not exhibit complete synchronization. The dark blue pattern on the diagonal in Fig. 4(c) implies that the spins around $i = 50$ exhibit oscillations close to phase difference 0° . Also, each spin exhibits 0° phase difference with the neighboring spins.

To validate the numerical results the frequency of the oscillations shown in Fig.3, obtained for the set of parameters $A = 2, B = 2, C = 1, K_z = 0.1, H_x = 0.1, H_y = 0, H_z = 0, \gamma = 1.0, \alpha = 0.005, j = 0.1, \beta = -0.6$, is analytically calculated. For this purpose, Eq. (4) is written in terms of cartesian coordinates as

$$\begin{aligned} \frac{dS_k^x}{dt} = & -A\alpha(1 - (S_k^x)^2)(S_{k-1}^x + S_{k+1}^x) + B(\alpha S_k^y S_k^x + \gamma S_k^z)(S_{k-1}^y + S_{k+1}^y) \\ & + C(\alpha S_k^z S_k^x - \gamma S_k^y)(S_{k-1}^z + S_{k+1}^z) - H_x\alpha(1 - (S_k^x)^2) \\ & + 2K_z S_k^z(\alpha S_k^x S_k^z - \gamma S_k^y) - j(1 - (S_k^x)^2), \end{aligned} \quad (6)$$

$$\begin{aligned} \frac{dS_k^y}{dt} = & A(\alpha S_k^x S_k^y - \gamma S_k^z)(S_{k-1}^x + S_{k+1}^x) - B\alpha(1 - (S_k^y)^2)(S_{k-1}^y + S_{k+1}^y) \\ & + C(\alpha S_k^y S_k^z + \gamma S_k^x)(S_{k-1}^z + S_{k+1}^z) + H_x(\alpha S_k^x S_k^y - \gamma S_k^z) \\ & + 2K_z S_k^z(\alpha S_k^y S_k^z + \gamma S_k^x) + j(S_k^x S_k^y + \beta S_k^z), \end{aligned} \quad (7)$$

$$\begin{aligned} \frac{dS_k^z}{dt} = & A(\alpha S_k^x S_k^z + \gamma S_k^y)(S_{k-1}^x + S_{k+1}^x) + B(\alpha S_k^y S_k^z - \gamma S_k^x)(S_{k-1}^y + S_{k+1}^y) \\ & - C\alpha(1 - (S_k^z)^2)(S_{k-1}^z + S_{k+1}^z) + H_x(\alpha S_k^x S_k^z + \gamma S_k^y) \\ & - 2K_z\alpha S_k^z(1 - (S_k^z)^2) + j(S_k^x S_k^z - \beta S_k^y). \end{aligned} \quad (8)$$

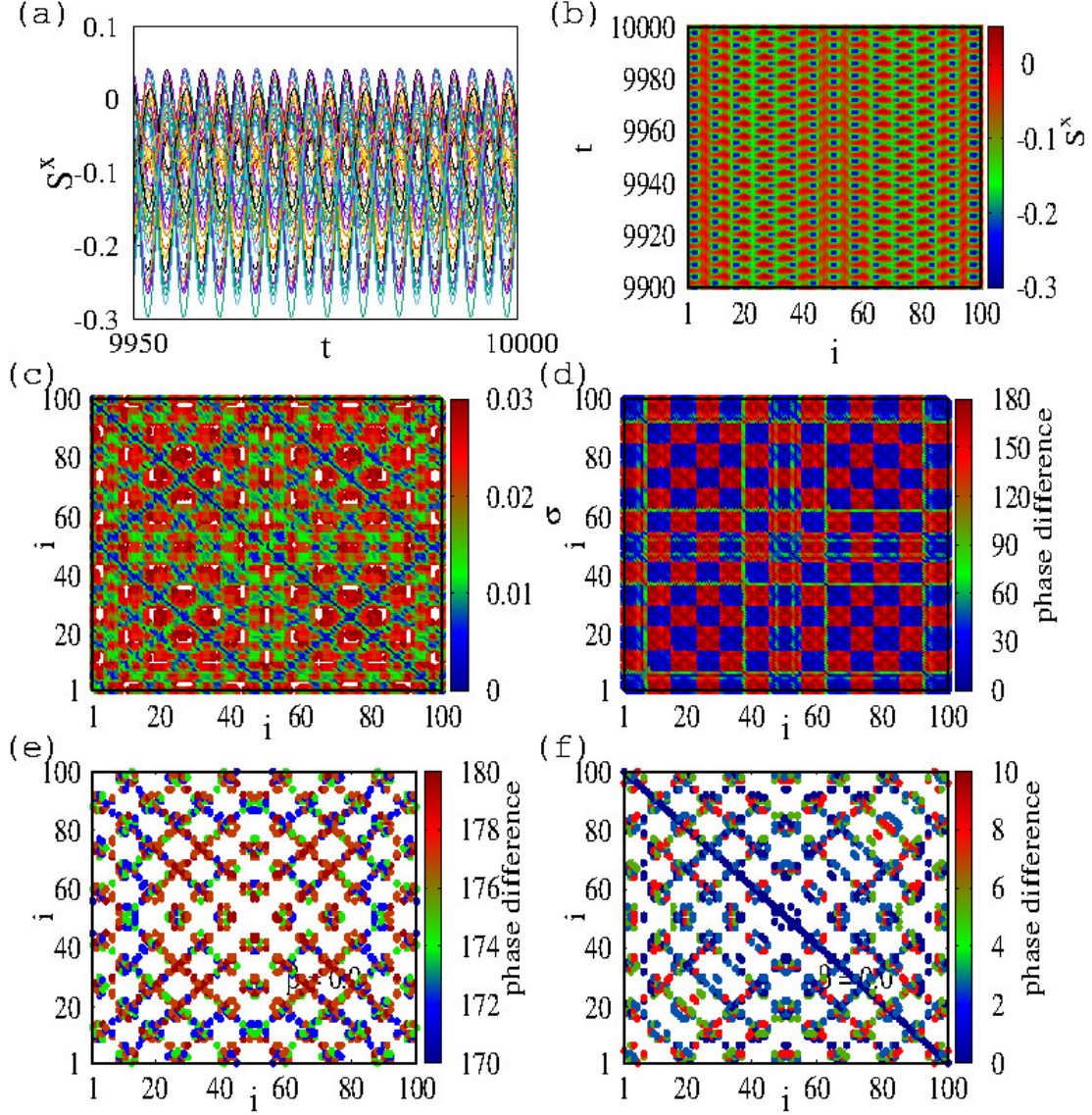


FIG. 6. (a,b) Time evolution of the spins, (c) standard deviation and (d-f) phase difference between the different pair of spins. Here, $H_x = 0.1, H_y = 0, H_z = 0.1, I = 0.1, \beta = -0.6$.

Using the transformations $S_k^x = \sin \theta_k \cos \phi_k$, $S_k^y = \sin \theta_k \sin \phi_k$, $S_k^z = \cos \theta_k$, we can derive the dynamical equation in terms of spherical polar coordinates as

$$\sin \theta_k \frac{d\phi_k}{dt} = \cos \phi_k \frac{dS_k^y}{dt} - \sin \phi_k \frac{dS_k^x}{dt}, \quad (9)$$

$$\sin \theta_k \frac{d\theta_k}{dt} = -\frac{dS_k^z}{dt}. \quad (10)$$

After substituting Eqs. (6)-(8) in Eqs. (9) and (10) we can obtain

$$\begin{aligned} \sin \theta_k \frac{d\phi_k}{dt} &= A(\alpha \sin \phi_k - \gamma \cos \theta_k \cos \phi_k)(\cos \phi_{k-1} \sin \theta_{k-1} + \cos \phi_{k+1} \sin \theta_{k+1}) \\ &\quad - B(\gamma \cos \theta_k \sin \phi_k + \alpha \cos \phi_k)(\sin \phi_{k-1} \sin \theta_{k-1} + \sin \phi_{k+1} \sin \theta_{k+1}) \\ &\quad + C\gamma \sin \theta_k(\cos \theta_{k-1} + \cos \theta_{k+1}) + H_x(\alpha \sin \phi_k - \gamma \cos \theta_k \cos \phi_k) \\ &\quad + K_z \gamma \sin(2\theta_k) + j(\beta \cos \theta_k \cos \phi_k + \sin \phi_k), \end{aligned} \quad (11)$$

$$\begin{aligned} \frac{d\theta_k}{dt} &= -A(\alpha \cos \theta_k \cos \phi_k + \gamma \sin \phi_k)(\cos \phi_{k-1} \sin \theta_{k-1} + \cos \phi_{k+1} \sin \theta_{k+1}) \\ &\quad + B(\gamma \cos \phi_k - \alpha \cos \theta_k \sin \phi_k)(\sin \phi_{k-1} \sin \theta_{k-1} + \sin \phi_{k+1} \sin \theta_{k+1}) \\ &\quad + C\alpha \sin \theta_k(\cos \theta_{k-1} + \cos \theta_{k+1}) - H_x(\alpha \cos \theta_k \cos \phi_k + \gamma \sin \phi_k) \\ &\quad + K_z \alpha \sin(2\theta_k) - j(\cos \theta_k \cos \phi_k - \beta \sin \phi_k). \end{aligned} \quad (12)$$

For the inphase synchronization it can be considered that $\phi_{k-1} = \phi_k = \phi_{k+1}$. Also from Fig. 5, which has been plotted for $S^z(t)$ corresponding to 100 number of spins, we can observe that the value of $S^z(t)$ for all the spins is approximately equal to 1. This indicates that $\theta_k \approx$ constant and $\cos \theta_k \approx 1$, $\sin \theta_k \approx \theta_k$ since $S_k^z = \cos \theta_k$. Hence, $\theta_{k-1} = \theta_k = \theta_{k+1}$. After using the above identities in Eq. (11) we can arrive at

$$\begin{aligned} \theta_k \frac{d\phi_k}{dt} &= \alpha(A - B)\theta_k \sin(2\phi_k) - 2\gamma\theta_k(A \cos^2 \phi_k + B \sin^2 \phi_k - C - K_z) \\ &\quad + (H_x \alpha + j) \sin \phi_k + (j\beta - H_x \gamma) \cos \phi_k. \end{aligned} \quad (13)$$

For the given set of parameters, $A = 2, B = 2, C = 1, K_z = 0.1, H_x = 0.1, H_y = 0, H_z = 0, j = 0.1, \gamma = 1.0, \alpha = 0.005, \beta = -0.6$, Eq. (13) can be written as

$$\theta_k \frac{d\phi_k}{dt} = -1.8 \theta_k + 0.1005 \sin \phi_k - 0.16 \cos \phi_k. \quad (14)$$

Integrating Eq. (14) with respect to ϕ_k from 0 to 2π , we get,

$$\theta_k \int_0^{2\pi} \frac{d\phi_k}{dt} d\phi_k = -1.8 \theta_k \int_0^{2\pi} d\phi_k + 0.1005 \int_0^{2\pi} \sin \phi_k d\phi_k - 0.16 \int_0^{2\pi} \cos \phi_k d\phi_k. \quad (15)$$

Here, $\frac{d\phi_k}{dt} = 2\pi f = \text{constant}$, where f is the frequency of the oscillations of the spins that exhibit inphase synchronized oscillations. Then the frequency is calculated from Eq. (15) as $|f| = 1.8/2\pi = 0.28$, which is exactly equal to the frequency of the oscillations plotted in Fig. 3, and this validates our numerical results.

B. Complete, inphase, antiphase and desynchronized oscillations

In the previous sections we observed that the field-like-torque causes the spins to oscillate in complete and inphase synchronization modes. Here we show that the spins can simultaneously exhibit complete, inphase, antiphase and desynchronization modes as well. Considering Figs. 6(a-f), we plot in Figs. 6(a-b) the time evolution of the 100 spins and in (c) the standard deviation between different spins and in (d-f) the phase difference between the different pairs of spins for $\beta = -0.6$. Here, the parameters are set the same as in Fig. 4 except that now $H_z = 0.1$. From the time evolution displayed in Figs. 6(a) and (b) we can observe that the spins oscillate with the character of antiphase synchronization. In addition to the antiphase synchronization the pair of spins $(i, N + 1 - i)$ exhibit complete synchronization. To confirm the complete synchronization between these pairs, the standard deviation (σ) is plotted between their values of $S^x(t)$ in Fig. 6(c), where we can see the pair of spins $(i, N + 1 - i)$ represented by the dark blue color exhibiting complete synchronized oscillations. To prove the existence of inphase and antiphase synchronization in the oscillations, the phase difference between all the pairs of spins among the 100 spins is plotted in Fig. 6(d), where the dark blue and red patterns confirm the regions of inphase and antiphase synchronized oscillations, respectively. Fig. 6(e) and (f) show that the spins oscillate with the phase difference of more than 170° and less than 10° , respectively, where the white region corresponds to the pairs of spins oscillating desynchronously with phase difference less than 170° and more than 10° , respectively. From Fig. 6 we can conclude that different groups of spins are exhibiting different kinds of oscillations, namely inphase, antiphase, complete and desynchronized oscillations. To get a clear visualization of the spins between which inphase, antiphase and complete synchronizations exist, in Fig. 7 we have plotted the pairs of spins corresponding to the phase differences $\sim 1^\circ$, $\sim 180^\circ$, and $\sigma < 0.001$, by bullets with colors red, blue and black, respectively. As we observed in Fig. 6, here it is exhibited that the pair of spins $(i, N + 1 - i)$ oscillate in complete synchronization.

Further, we can show the possibility of antiphase synchronized oscillations between the pairs $(i, N + 1 - i)$ instead of inphase synchronization for the values of fields $H_x = 0.1, H_y = 0.2, H_z = 0.3$. The time evolution is plotted in Figs. 8(a) and (b), where the antiphase nature is clearly visible. In Fig. 8(c) the phase difference is plotted for different pairs of spins with different color shades, which confirms the existence of inphase, antiphase and

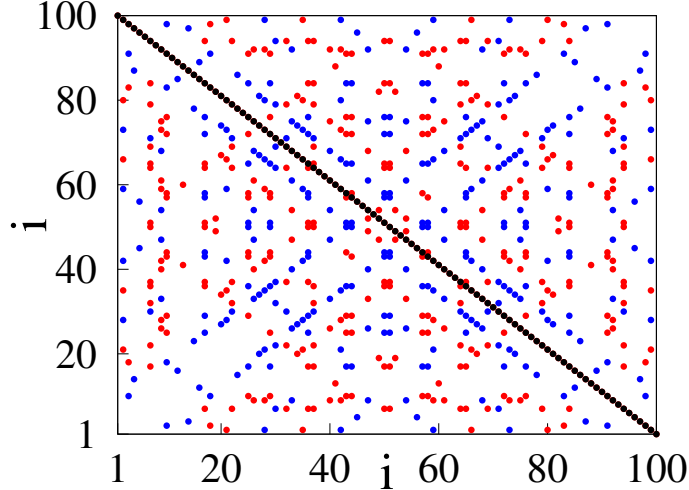


FIG. 7. The pair of spins exhibiting inphase ($\sim 1^\circ$), antiphase ($\sim 180^\circ$), complete synchronized ($\sigma < 0.001$) oscillations are plotted with red, blue and black bullets, respectively. Here, $H_x = 0.1, H_y = 0, H_z = 0.1, j = 0.1, \alpha = 0.005, \beta = -0.6$.

desynchronized oscillations. Also, the spins exhibiting inphase, antiphase and complete synchronization are plotted with red, blue and black bullets, respectively in Fig. 8(d).

IV. CONCLUSIONS

We have numerically simulated the dynamics of spins in a one-dimensional anisotropic Heisenberg ferromagnetic spin chain for their different modes of self-oscillations by solving Landau-Lifshitz-Gilbert-Slonczewski equation numerically. The dynamical equation for the ' k '-th spin has been written from the Hamiltonian corresponding to the N number of spins. The self-oscillations in spins are achieved for the specific values of external field and current. It is shown that when the number of spins becomes large the synchronization is lost between them and they oscillate desynchronously. However, the synchronization can be restored with the inclusion of field-like torque and we have proved the simultaneous existence of inphase and complete synchronization in the oscillations. The complete synchronization is shown between the pair of spins $(i, N + 1 - i)$, which has been confirmed by plotting standard deviation between their oscillations. Additionally, we have confirmed the coexistence of inphase, antiphase, complete and desynchronized modes of oscillations among the spins when the magnetic field is applied in both directions x and z . Further, we have shown that

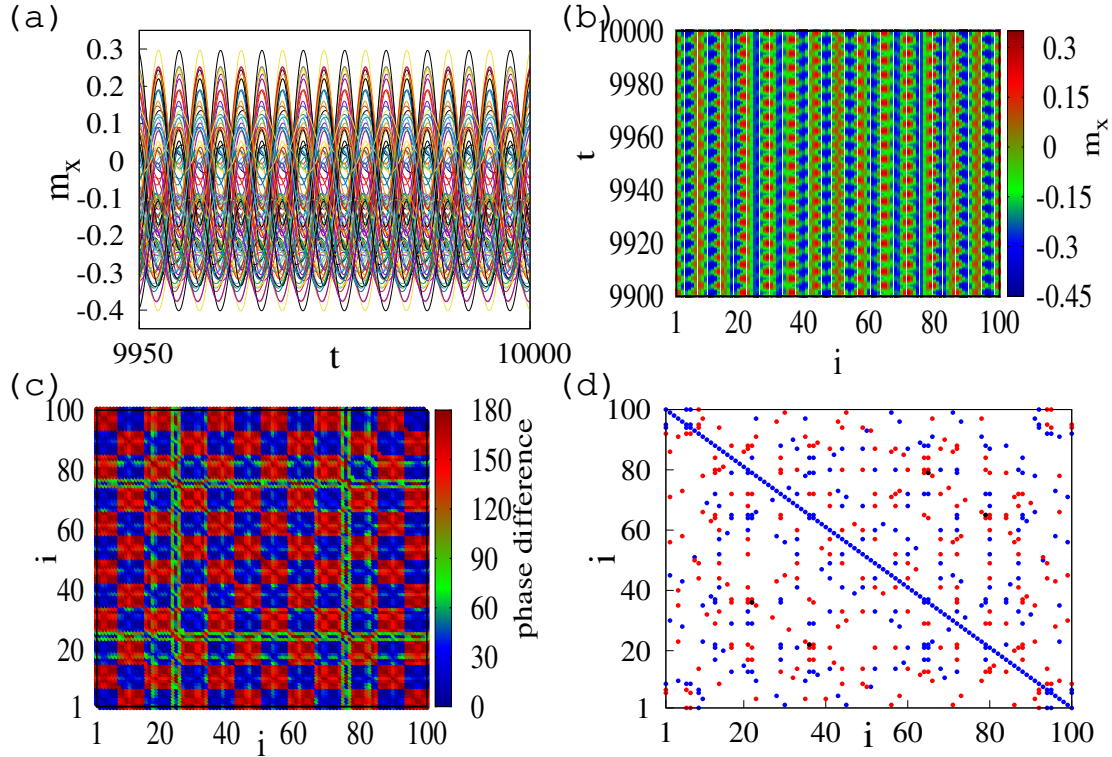


FIG. 8. (a,b) Time evolution of the spins, (c) Phase difference between the different pairs of spins, and (d) inphase (red), antiphase (blue), and complete synchronization (black). Here, $H_x = 0.1$, $H_y = 0.2$, $H_z = 0.3$, $I = 0.1$, $\beta = -0.6$.

the antiphase synchronization between the pairs $(i, N + 1 - i)$ occurs instead of complete synchronization by applying the field in all the directions x , y , and z . The frequency of the inphase synchronized oscillations is analytically derived and it matches with the numerical values.

ACKNOWLEDGMENTS

M.L. wishes to acknowledge the ANRF award of a ANRF-SERB National Science Chair under Grant No. NSC/2020/00029. R.A. would like to thank SRM TRP Engineering College, India, for their financial support, vide number SRM/TRP/RI/005. Work of A.S. was supported by the U.S. Department of Energy.

AUTHOR DECLARATIONS

Conflict of Interest

The authors have no conflicts to disclose.

DATA AVAILABILITY

The data that support the findings of this study are available from the corresponding author upon reasonable request.

REFERENCES

- ¹M. Lakshmanan, Phys. Lett. A **61**, 53 (1977).
- ²L. Takhtajan, Phys. Lett. A **64**, 235 (1977).
- ³V. Zakharov and L. Takhtajan, Theoret. Math. Phys. **38**, 17 (1979).
- ⁴A. S. Borovik-Romanov, Solid State Commun. **34**, 721 (1977).
- ⁵K. Nakamura and T. Sasada, J. Phys. C **15**, L915 (1982).
- ⁶E. K. Sklyanin, LOMI preprint **E-3-79** (1979).
- ⁷Y. Ishimori, Prog. Theor. Phys. **72**, 33 (1984).
- ⁸M. Lakshmanan and A. Saxena, Physica D **237**, 885 (2008).
- ⁹A. J. Sievers and S. Takeno, Phys. Rev. Lett. **61**, 970 (1988).
- ¹⁰Y. Zolotaryuk, S. Flach, and V. Fleurov, Phys. Rev. Lett. **91**, 214101 (2003).
- ¹¹A. Sievers and S. Takeno, Phys. Rev. Lett. **61**, 970 (1988).
- ¹²J. B. Page, Phys. Rev. B **41**, 7835 (1990).
- ¹³D. K. Campbell, S. Flach, and Y. S. Kivshar, Phys. Today **57**, 43 (2004).
- ¹⁴S. Flach and C. R. Willis, Phys. Rep. **295**, 181 (1998).
- ¹⁵R. S. MacKay and S. Aubry, Nonlinearity **7**, 1623 (1994).
- ¹⁶S. Aubry, Physica D **103**, 201 (1997).
- ¹⁷S. V. Rakhmanova and A. V. Shchegrov, Phys. Rev. B **57**, R14012 (1998).
- ¹⁸Y. Zolotaryuk, S. Flach, and V. Fleurov, Phys. Rev. B **63**, 214422 (2001).
- ¹⁹A. V. Savin, J. M. Khalack, P. L. Christiansen, and A. V. Zolotaryuk, Phys. Rev. B **65**, 054106 (2002).
- ²⁰R. Lai and A. J. Sievers, J. Appl. Phys. **81**, 3972 (1997).
- ²¹L. Q. English, M. Sato, and A. J. Sievers, Phys. Rev. B **67**, 024403 (2003).
- ²²J. P. Nguenang, M. Peyrard, A. J. Kenfack, and T. C. Kofane, J. Phys. Condens. Matter **17**, 3083. (2005).
- ²³M. Lakshmanan, R. Arun, and A. Saxena, Physica A **584**, 126319 (2021).
- ²⁴M. Lakshmanan and A. Saxena, Physics Letters A **382**, 1890 (2018).